A Monte Carlo Simulation on the Effects of Chain End Modification on Freely Standing Thin Films of Amorphous Polyethylene Melts

Jee Hwan Jang,[†] Rahmi Ozisik,[†,‡] and Wayne L. Mattice*[,†]

Institute of Polymer Science, University of Akron, Akron, Ohio 44325-3909, and Institut fur Polymere, ETH Zentrum, Zurich, CH-8092, Switzerland

Received May 31, 2000; Revised Manuscript Received July 31, 2000

ABSTRACT: The effects of chain end modification on freely standing amorphous polyethylene thin films with a thickness $2R_g$ to $4R_g$ (radius of gyration) are studied by a Monte Carlo (MC) simulation on a high coordination lattice. The rotational isomeric state (RIS) model is incorporated into the simulation as short-range interactions, and a Lennard-Jones (LJ) potential is used to calculate the long-range interactions. The modification of the chain ends is introduced by changing the well-depth (ϵ) of the LJ potential as compared to the middle beads. Chain ends with $\epsilon_{end} \leq \epsilon_{middle}$ show segregation near the free surface, but chain ends with $\epsilon_{end} \gg \epsilon_{middle}$ prefer to remain in the bulklike region. Both entropy and enthalpy are major factors in the determination of the distribution of the chain ends. The effects of the free surface can extend farther than R_g into the interior of the thin film. However, for the case of relatively attractive chain end (ϵ_{end} slightly larger than ϵ_{middle}), a fairly large length of isotropic region is observed at the molecular level due to the balance of the entropic effect to prefer a free surface and the enthalpic effect to prefer bulk region. The repulsive chain ends ($\epsilon_{end} < \epsilon_{middle}$) induce faster dynamics in the middle region of the film as observed by the center-of-mass displacement and the chain shape autocorrelation function.

Introduction

The end groups of a polymer chain are different from the middle groups in terms of their chemical nature and chain connectivity. The understanding of this difference is crucial in the explanation of the change of static and dynamic properties incurred by modification of the chain ends. The effect of the chain end was phenomenologically introduced in the reptation model.[1,2] A recent study[3] on a series of *n*-alkanes by the pulsed-gradient spin-echo NMR experiment infers a larger free volume around the chain ends. This free volume was successfully parametrized to obtain a semiempirical density equation as a function of the molecular weight. Additionally, the larger free volume causes greater mobility near the chain ends, which was observed by Horinaka et al.[4] in the fluorescence depolarization of the oligo- and polystyrene chain ends. The glass transition temperature (T_g) is also affected by the chain ends; T_g decreases with decreasing molecular weight.[5]

While the larger free volume of the chain ends may account for the entropic origin of the end group effect, the chemical nature of the chain ends can provide an enthalpic origin. Therefore, if a heterogeneous boundary is applied to a bulk system to generate a surface or an interface, the location of the chain ends is determined by the balance of the two thermodynamic factors. Elman et al.[6] directly observed the different distribution of chain ends by neutron reflectometry on end-functional polystyrene. The different chain end composition in a surface compared to that in the bulk region would lead to a change in the surface properties. Mayes[7] derived a scaling relation for T_g reduction at the polymer−vacuum surface, and Kajiyama et al.[8] observed the reduction of T_g at the polystyrene film surface by scanning force microscopy and lateral force microscopy measurements. The reduction in T_g was attributed to the excess free volume generated by the segregation of the chain ends at the surface, which lowers the entropic penalty. However, Tanaka et al.[9] observed a glassy behavior on the α,*ω*-polystyrene (COOH) and α,*ω*-polystyrene (NH_2) at a certain temperature, while unfunctionalized polystyrene showed a glass−rubber transition at the same temperature. This elevation of T_g was attributed to the depletion of the chain ends at the surface due to the higher surface energies of the −COOH and $-NH_2$ groups. The surface tension also depends on the chemical nature of the chain ends, as was shown by pendent drop tensiometry on poly(dimethylsiloxane) with various chain ends.[10] The dependence of the surface properties on the chemical nature of the chain ends has drawn attention to finding practical applications like thermally stable polymer thin films,[11] A−B/A block copolymeric systems,[12] stable micelles of amphiphilic block copolymers,[13] and self-healing surface.[14]

Despite the increased interest in the surface modification by introducing different chain ends, the understanding of the chain end effect near a surface at the molecular level is incomplete largely due to the experimental difficulties in sample preparation. The previous theoretical and simulation studies rely on the mean field treatment or on coarse-grained models. The coarse-grained models are sometimes sufficient to describe the large size and long time behavior of the polymeric systems, even though molecular description and the molecular behavior are necessary for a thorough understanding of the chemically modified system. However, a fully atomistic system cannot be simulated with the current computational resources because of the tremendous number of degrees of freedoms it contains.

A coarse-grained Monte Carlo simulation on a high coordination lattice has been developed to explore the behavior of the large polymeric systems. The model incorporates the rotational isomeric state (RIS) theory, which gives the molecular detail depending on the level of coarse-graining, and long-range interaction which

[†] University of Akron.
[‡] ETH Zentrum.

10.1021/ma000957m CCC: $19.00
Published on Web 09/07/2000

would be essential to describe the large-scale properties of the system. The simulation method has been validated in the previous studies on freely standing films,[15] thin films attached to an attractive solid wall,[16] and thin films in a confined geometry[17] producing reasonable static and dynamic properties with good agreement to experimental observations.

This paper focuses on one of the mechanisms of chain end modification on the static and dynamic properties of thin films at the molecular level. Specifically, we examine the effect of a different intermolecular attraction (represented by ϵ in a Lennard-Jones potential energy function) for end groups than for internal groups. Differences in size (which would require different σ in the Lennard-Jones potential energy function) are not included, nor do we include any differences in the short-range intramolecular interaction expressed in a rotational isomeric state model. The simulations are designed to investigate the intermolecular consequence of the chain ends having different dispersive attraction than the internal groups.

Computations

The detailed description of the lattice structure, the energetics, and the single bead moves for the present simulation were described elsewhere.[18−20] A linear polyethylene chain can be mapped onto the tetrahedral lattice with a fixed bond length of 1.53 Å and a fixed bond angle of 109.5°. In this mapping, each lattice site represents a single $-CH_2-$ or $-CH_3-$ group on the polyethylene chain. The bond between two neighboring lattice sites can be in one of three rotational states; trans (t), gauche$^+$ (g^+), or gauche$^-$ (g^-). If the chain is more coarsely represented by deletion of every second carbon atom, it can now be placed on a coarse-grained lattice obtained by discarding every second site from the tetrahedral lattice. This coarse-grained lattice provides a better computational efficiency due to the reductions in the number of particles and in the number of conformational states, which facilitates its application to fairly large polymeric systems. The coarse graining generates a slanted cubic cell, identical to the closest packing of uniform hard spheres, whose length is 2.5 Å in *a*, *b*, and *c* directions, and the angles between any two unit vectors are 60°. The modification produces a higher coordination number than that of the tetrahedral lattice. The molecular description of the beads and the rotational states of the virtual bonds between two neighboring lattice sites are also changed. Each internal bead in this model represents an ethylene ($-CH_2-CH_2-$) group. Since two C−C bonds are embedded in the virtual bond, the rotational isomeric states between i and $i + 2$ beads should represent two successive rotational states in a real chain.

The rotational isomeric states between i and $i + 2$ beads can be categorized into four groups, which are specified by the distances between these two beads. The distances of 5.00, 4.33, 3.53, and 2.50 Å correspond to the local conformations of A: tt, B: (tg^+,tg^-,g^+t,g^-t), C: (g^+g^+,g^-g^-), and D: (g^+g^-,g^-g^+), respectively. Exploring the local conformational space during equilibration or relaxation requires the determination of energetics based on the rotational states, which eventually enters the Metropolis[21] evaluation. Technically, this is done by determining the probability and the conditional probability for the rotational states through the rotational isomeric states (RIS) formalism.[22] We adopt the conventional RIS model for polyethylene of Abe et al.[23] with the statistical weight matrix

$$U_{\text{polyethylene}} = \begin{pmatrix} 1 & \sigma & \sigma \\ 1 & \sigma & \sigma\omega \\ 1 & \sigma\omega & \sigma \end{pmatrix} \tag{1}$$

where σ and ω are the first- and the second-order interaction parameters and the rows are indexed by the states of $(i-1)$th bond and the columns are indexed by the states of ith bond. The orders of indexing are t, g^+, and g^-. The short-range intramolecular interactions in this 3×3 matrix, written for a C−C bond of length 1.53 Å, are mapped onto the description of the coarse-grained chain, using a 9×9 matrix for the internal bond of length 2.50 Å.

The incorporation of the rotational isomeric state model is not enough to describe the energetics of the melt system because the RIS model is a single chain model. The model only accounts for the short-range intramolecular interaction up to next-nearest-neighbor bonds on the 2nnd lattice. For the remaining long-range intramolecular interactions and all intermolecular interactions, the Lennard-Jones pair potential, $u(r)$, seems to be a reasonable choice since there are only dispersive interactions in a polyethylene melt. The lattice representation of the continuous Lennard-Jones potential at the ith shell, u_i, is obtained from an averaged Mayer f-function.[19] The interaction parameter at the ith shell is defined through the following equation.

$$\exp\left(-\frac{u_i}{k_B T}\right) - 1 \equiv \bar{f}_i \tag{2}$$

The average Mayer f-function at the ith shell, f_i, is obtained by integrating $u(r)$ over the cells in the ith shell.

$$\bar{f}_i = \frac{\int_{\text{cell}} f \, \mathrm{d}r}{\int_{\text{cell}} \mathrm{d}r} \tag{3}$$

$$f = \exp\left(-\frac{u(r)}{k_B T}\right) - 1 \tag{4}$$

The set of interaction parameters for the middle beads, $\{u_i^{\text{middle}}\}$, is derived from the Lennard-Jones potential for ethylene ($CH_2{=}CH_2$) which has $\epsilon/k_B = 205$ K and $\sigma = 4.2$ Å. For the modification of the chain end, several different ϵ values and $\sigma = 4.2$ Å are used for the derivation of the interaction parameters. This modification can model the effect of the change of chemical nature at the chain end. When $\epsilon > 205$, the chains are terminated with more attractive chemical groups than the backbone. For the interaction parameters between a middle bead and an end bead, the Lorentz−Berthelot geometric average, $\epsilon_{AB} = (\epsilon_A \epsilon_B)^{1/2}$, is used. Only the first three $u_{i,i=1-3}$ are used for the computational efficiency, implying a cutoff distance of 7.5 Å in the long-range interaction.

The single bead move is employed in the simulation with the restriction that a chain cannot pass through itself, as in a self-avoiding random walk. A randomly chosen bead can move to a vacant site in the first shell when the attempt does not change the bond length to its bonded neighbors. One Monte Carlo step (MCS) is

Table 1. Simulation Parameters

run	chain	no. of chains	temp (K)	ϵ/k of end bead (K)
I-1	C60	32	443	205
I-2	C60	64	443	205
I-3	C60	128	443	205
II-1	C80	24	503	100
II-2	C80	24	503	205
II-3	C80	24	503	300
II-4	C80	24	503	350
II-5	C80	24	503	500
II-6	C80	24	503	600
III-1	C80	48	503	100
III-2	C80	48	503	205
III-3	C80	48	503	350
III-4	C80	48	503	600

defined as the simulation length when every bead in the system has attempted one move, on average.

For the generation of freely standing films, first their bulk states are constructed and equilibrated. The equilibration of the bulk systems is divided into two stages according to the applied energetics. First, only short-range interaction is applied during several million MCS to remove any bad contacts that existed in the initial bulk structures built randomly. Second, the long-range interactions of middle bead−middle bead, middle bead−end bead, and middle bead−end bead are added to the evaluation of energetics in further equilibration. After the equilibration with the long-range interaction on the bulk system, the *z* directional periodic condition in the bulk is removed by expanding the *z* periodicity to generate *xy* directional free surfaces at both sides. This simple method[24] called "elongation or expansion method" has been a successful way to generate freely standing films with a well-defined free interface.[15] After equilibration of the freely standing films with different long-range interactions for the end beads, static and dynamics properties of the film are analyzed. Table 1 summarizes the simulation parameters used in this work.

All computations were carried out using a R10000 Silicon Graphic workstation. Approximately 200 h of CPU time was consumed for the generation, the relaxation, and the data gathering for each thin film of category III in Table 1.

Results and Discussion

Thickness Requirement in the Free-Standing Films. The smallest acceptable size for our simulation is determined by the anticipated length scale of the special environment of the surface of the film. In an earlier simulation of an atomistic description of a freely standing thin films,[25] the interfacial width deduced from the density profile was found to be around a few monomer units. The effective range of a solid wall during the interdiffusion process was shown by Lin et al.[26] to be around $3-4R_g$, when R_g is the radius of gyration of a chain. The effect can extend over the contour length of the polymer as shown in the diffusion experiments of Frank et al.[27]

To find out the thickness requirement in our simulation, three C_{60} thin films were produced with three different thickness values: $\sim 2R_g$, $\sim 4R_g$, and $\sim 8R_g$, where R_g is around 11 Å in the bulk. Figure 1 shows the density profiles normal to the surface of the three films at 443 K. The densities were obtained from counting the beads as a function of distance from the center of the film and averaging over all configurations in the simulation. The density profiles were fitted with

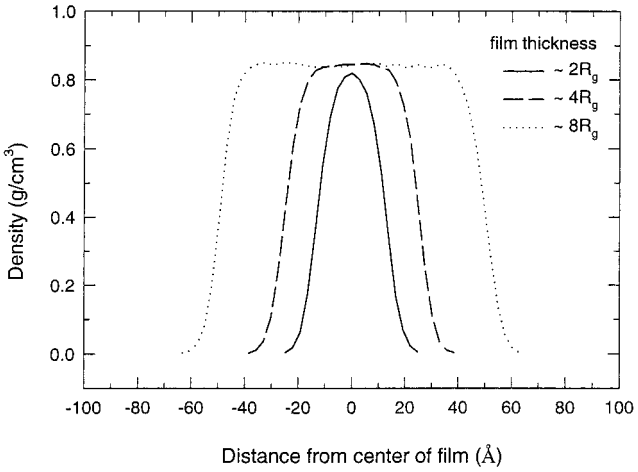

Figure 1. Density profiles of the linear C_{60} polyethylene freely standing films of different thickness at 443 K against the distance from the center of film. The solid, dashed, and dotted lines correspond to the films containing 32, 64, and 128 chains of C_{60}, respectively.

Table 2. Fit of the Hyperbolic Interfacial Equation, Eq 5, to the Density Profiles of C60 Amorphous Polyethylene Freely Standing Films at 443 K (Figure 1)

thickness[a]	ρ_{bulk} (g/cm^3)	h (Å)	w (Å)
$\sim 2R_g$	0.824 ± 0.006	12.62 ± 0.08	11.50 ± 0.27
$\sim 4R_g$	0.843 ± 0.003	24.93 ± 0.07	11.41 ± 0.23
$\sim 8R_g$	0.843 ± 0.002	49.78 ± 0.07	12.90 ± 0.26

[a] The values are approximated by the mean radius of gyration of C60 chains in the bulk, which is around 11 Å.

a hyperbolic equation, which was originally developed by Helfand and Tagami[28,29] for the interface in immiscible binary blends.

$$\rho(z) = \rho_{bulk}\frac{1 - \tanh[2(z-h)/w]}{2} \qquad (5)$$

Here ρ_{bulk} is the density of the middle region of the film (the center), h is the location of the interface, w is the interfacial width, and z is the distance from the center of mass of the film. This hyperbolic equation fits the density profiles of the free-standing thin films very well with the parameters in Table 2. The ρ_{bulk} values of the two thicker films are almost the same, but the ρ_{bulk} of the thinnest film is significantly lower than those of the other two films. For further simulation of a large bulk system, the ρ_{bulk} of the thicker film can be considered as a bulk density. This result is an indication that film should be thicker than $4R_g$ to have a stable middle region that is not affected by the free surface. Obviously this statement is based on the density considerations only.

In addition to the static properties, the dynamic properties are also perturbed by the existence of a surface. The effective region of the perturbation has a limited length, which could be related to the size of the chain or the molecular weight. If the perturbation is strong enough, as with a very attractive solid wall,[30] the effect can extend over the contour length of the chain due to the fixed contact of the chain at the solid wall. The change in the dynamic properties of a freely standing thin film of C60 was also investigated. The bottom panel of Figure 2 shows the two different short-time diffusivities of the chains vs the initial position of

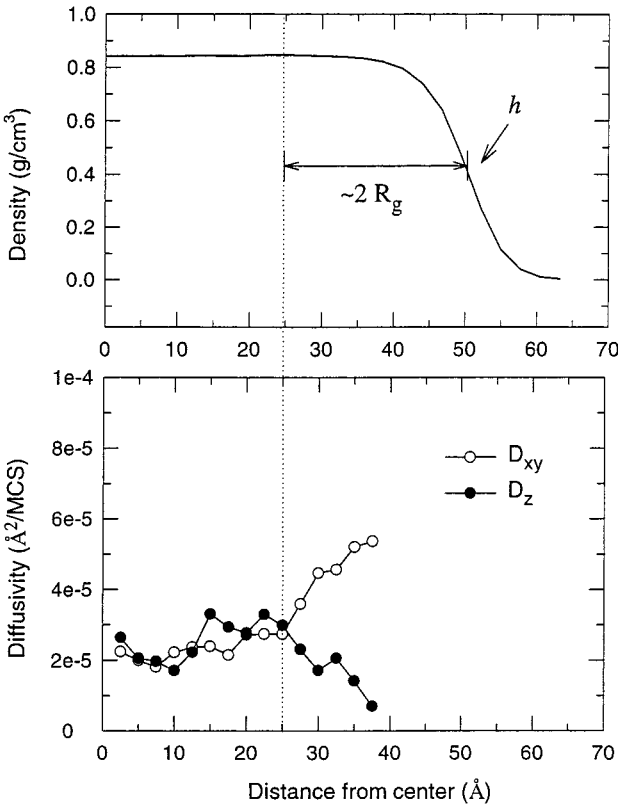

Figure 2. (a) Density profile of the freely standing films composed of 128 C_{60} linear polyethylene chains at 443 K. The arrow indicates the location of interface, *h*, obtained from a curve fitting of eq 5. (b) The short-time diffusivities in the lateral direction to the film surface (○) and in the normal direction to the film surface (●) as a function of the distance from the center of film.

the center of mass of the chains in the thin film, which were calculated according to the following equations:

$$D_{xy} = \frac{\sum_{i=0}^{N}\{[x_{CM}(t+i) - x_{CM}(0+i)]^2 + [y_{CM}(t+i) - y_{CM}(0+i)]^2\}}{4t(N+1)} \quad (6)$$

$$D_z = \frac{\sum_{i=0}^{N}\{z_{CM}(t+i) - z_{CM}(0+i)\}^2}{2t(N+1)} \quad (7)$$

Here, $N + 1$ denotes the total number of conformations for the ensemble average, and the dimension of the time unit is the Monte Carlo step (MCS). The true diffusion coefficients, taken as the limit at infinite time, must be independent of the initial coordinates of the center of mass of the chain. To retain memory of the initial coordinates, we truncate the trajectory so that the approximation to D_{xy} and D_z depends on the initial distance from the center of the film. The short-time approximation to the lateral diffusion constant (D_{xy}) and the normal diffusion constant (perpendicular to the surface, D_z) are not very different in the middle region of the film. The two diffusivities start to deviate at a distance of around $2R_g$ from the interface. This is another indication that a film thickness greater than $4R_g$ is necessary to have a bulk region. This result agrees with the one obtained from the density considerations.

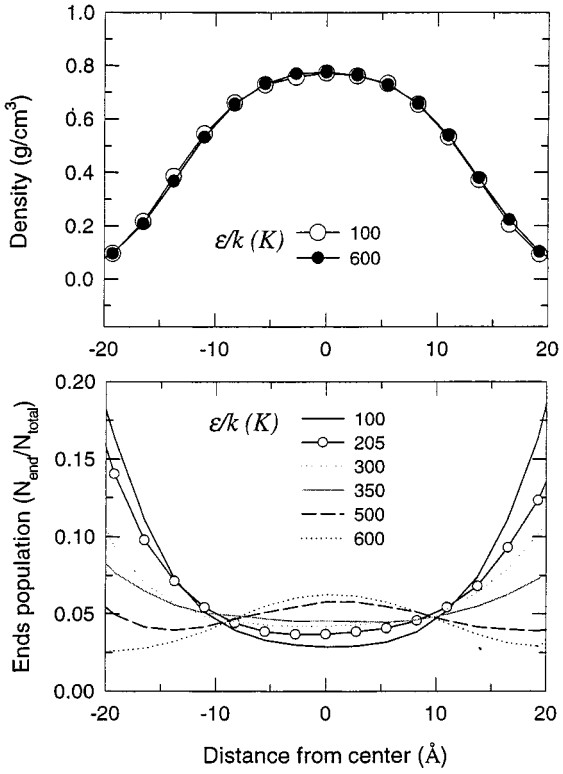

Figure 3. (a) Density profiles of freely standing films composed of 24 linear C_{80} polyethylene chains with modified chain ends at 503 K. The numbers 100 (○) and 600 (●) represent the ϵ values of Lennard-Jones potential which are used for the pair interaction between an end bead and an end bead. (b) The chain end population in the freely standing films against the distance from the center of film. A series of the ϵ values are used for the pair interaction between two end beads. The pair interaction between two middle beads uses $\epsilon = 205$.

Very Thin Films with Modified Chain Ends. We also investigated the effect of the film thickness on the chain end modification. The freely standing films were built from 24 chains of C80 at 503 K. The thickness of this system is about $2R_g$. The chain end modification is introduced by using a different set of parameters for end bead−end bead, end bead−middle bead, and middle bead−middle-bead interactions as explained in the previous section. It is seen that the density profiles are similar irrespective of the chain ends modification, as shown in Figure 3a. On the other hand, the distribution of the chain ends is strongly dependent on the chain end modification. The thin films with the least attractive chain ends ($\epsilon = 100$) have a distribution profile that shows a strong segregation of chain ends near the free surface. The strength of the segregation decreases as the chain ends are modified to be more attractive. If the chain ends are sufficiently attractive ($\epsilon = 500$ and 600), the film shows a depletion of the end groups near the free surface while it shows a segregation in the middle region. In the case of $\epsilon = 205$, where all three interactions (end−end, end−middle, and middle−middle) are the same, a segregation that is similar to the $\epsilon = 100$ case is observed. For $\epsilon = 300$ and 350, an enrichment of the end groups was also observed near the free surface.

If the chain end is much more effective than the internal beads at participating in attractive intermolecular interactions, which occurs in this simulation when the ends have $\epsilon \geq 500$, the ends move to the interior of the film, where there are more opportunities

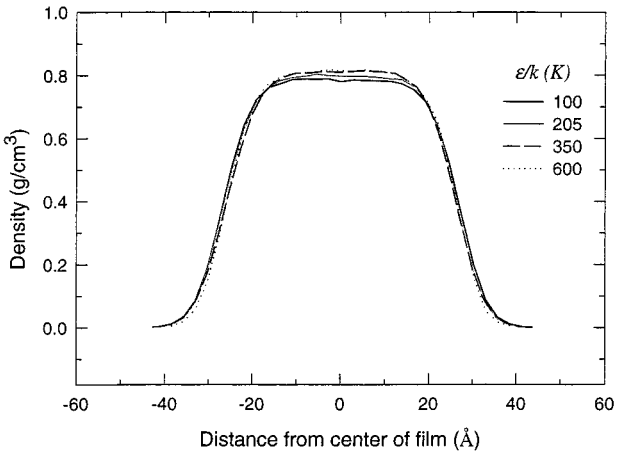

Figure 4. Density profiles of the freely standing films composed of 48 linear C_{80} polyethylene chains at 503 K. Four different ϵ values, 100 (solid line), 205 (gray line), 350 (dashed line), and 600 (dotted line), are used for the pair interaction between two end beads.

Table 3. Fit of the Hyperbolic Interfacial Equation, Eq 5, to the Density Profiles of the C80 Amorphous Polyethylene Freely Standing Films with Different Chain Ends at 503 K (Figure 4)

ϵ/k (K)[a]	ρ_{bulk} (g/cm^3)	h (Å)	w (Å)
100	0.782 ± 0.002	26.82 ± 0.06	12.49 ± 0.20
205	0.796 ± 0.002	26.37 ± 0.05	12.22 ± 0.17
350	0.808 ± 0.003	26.22 ± 0.07	12.02 ± 0.24
600	0.810 ± 0.004	26.18 ± 0.10	11.72 ± 0.35

[a] The values represent the ϵ parameters of Lennard-Jones potential for the interaction between two end beads. For the interaction between two middle beads, $\epsilon = 205$ is used, and for the interaction between an end bead and a middle bead, the geometric average $\epsilon_{AB} = (\epsilon_A\epsilon_B)^{1/2}$ is used.

for their attractive interaction. This situation provides a higher packing around the chain ends, thereby reducing their free volume. Conversely, the free volume around a chain end will increase when its value of ϵ decreases. The chain end itself has a tendency to migrate to the surface due to the greater free volume of the chain end relative to the middle group, which is considered to be an entropic effect. The chain ends have less entropic penalty in a less crowded free surface region.

Films with Thickness Close to $4R_g$. It was seen in the previous sections that the different chain end distribution observed under various end bead modifications does not change the density profiles for the thin films with a of thickness $\sim 2R_g$. When the film thickness is increased, the density in the middle of the film shows a clear dependence on the nature of the chain end as shown in Figure 4. Table 3 gives the optimized parameters of the curve fitting of the density profiles to eq 5. The attractive chain ends bring other beads into the middle region, which creates a higher density compared to the that of the nonmodified film. Figure 5 shows the chain end distribution in the thick film under various chain end modification conditions. As is the case for thin films, the repulsive ends prefer to go to the free surface, and only the sufficiently highly attractive chain ends show a depletion near the free surface. Table 3 shows that the values of w increase when the free ends are segregated at the surface. Another interesting feature in the thick film is the oscillation of the chain end population, seen upon close examination of Figure 5. The periodicity of the oscillation is around $\sim 2R_g$. This

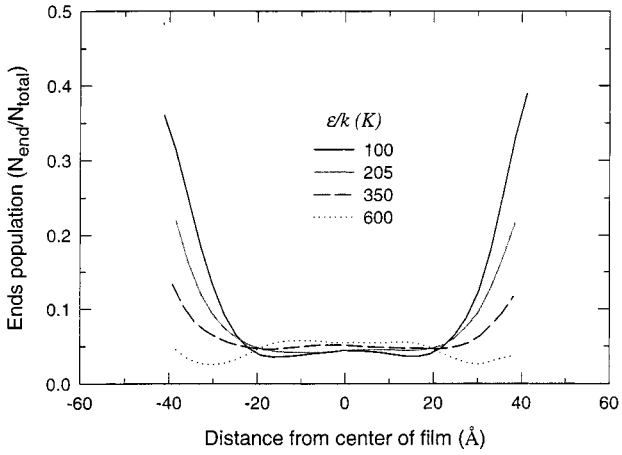

Figure 5. Chain ends population in the freely standing films composed of 48 amorphous linear C_{80} polyethylene chains at 503 K against the distance from the center of film. Four different ϵ values, 100 (solid line), 205 (gray line), 350 (dashed line), and 600 (dotted line), are used for the pair interaction between two end beads.

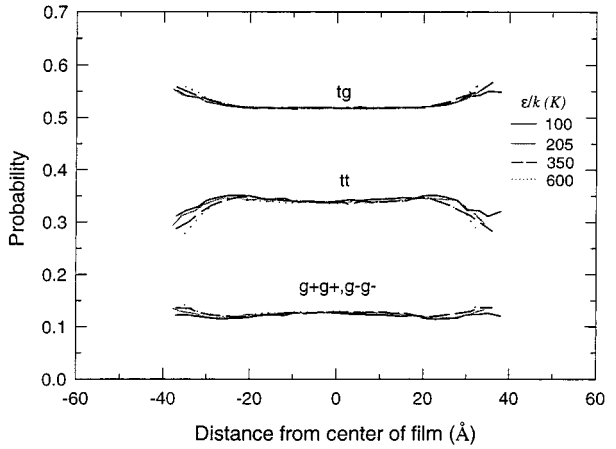

Figure 6. Probability of the local conformation for the freely standing films composed of 48 amorphous linear C_{80} polyethylene chains with modified chain ends at 503 K against the distance from the center of the films. The *tt*, *tg*, and g^+g indicate *tt*, (tg^+,tg^-,g^+t,g^-t), and (g^+g^+,g^-g^-), respectively. The probability for (g^+g^-,g^-g^+) is not shown due to its small contribution.

observation agrees with the theoretical prediction.[30]

Several works[30−32] have dealt with a surface near a hard wall or in a confined geometry by adopting an incompressible model, which gives a constant density in the system. In the incompressible system, the free energy contribution driven by the entropy change is restricted, and hence the role of the enthalpic contribution is expected to be the major factor in the determination of the system properties. Jalbert et al.[10] found that the segregation of the chain ends was largely controlled by the energetic difference between the chain ends and the middle groups. The freely standing film in the current model, which is compressible, accounts for the two thermodynamic contributions. As shown in Figure 5, the chains with nonmodified ends and even the weakly attractive chain ends are segregated near the free surface. The segregation is explained by the free volume effect based on the entropic contribution of the chain ends. The entropic contribution is overcome when the chain ends are sufficiently attractive, giving a depletion at the free surface as in the case of $\epsilon = 600$.

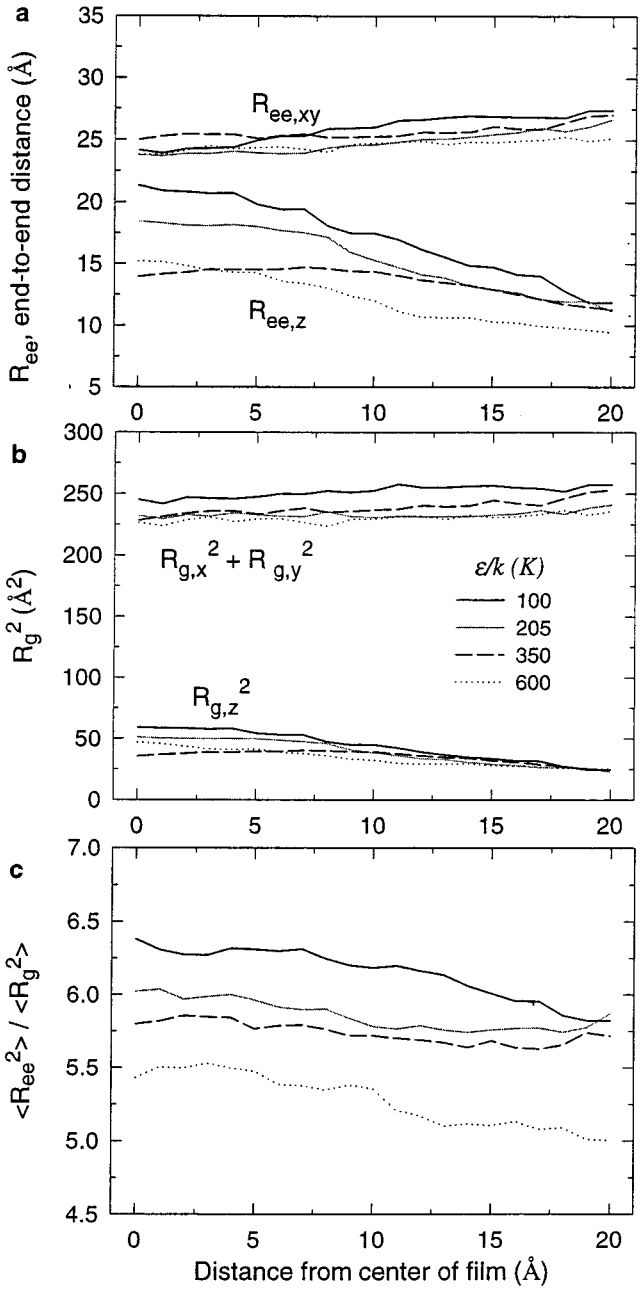

Figure 7. (a) The *xy* and *z* components of the end-to-end distance against the distance from the center of mass of the films. (b) The components of the mean-squared radius of gyration. (c) The ratio of mean-squared end-to-end distance to the mean-squared radius of gyration. In all figures, four different ϵ values, 100 (solid line), 205 (gray line), 350 (dashed line), and 600 (dotted line), are used for the pair interaction between two end beads.

Figure 6 presents the probabilities of the distinguishable pairs of isomeric states at two consecutive C−C bonds. The population is in the order (tg^+,tg^-,g^+t,g^-t) > tt > (g^+g^+, g^-g^-) > (g^+g^-,g^-g^+). The high population of gauche states in the free surface region can be easily explained by considering the chain end depletion, which results in collapsed conformations. The population of (g^+g^-,g^-g^+) is not shown in Figure 6 and is very small due to the unfavorable pentane effect.[23] In the middle region of the film, the probabilities do not vary much with the chain end modification. However, in the free surface region, the chains with attractive chain ends are more likely to be in the gauche state. The chains with attractive chain ends are in a higher energy state than the chains with repulsive chain ends due to the high population of gauche states. Jalbert et al.[10] observed high surface tension at low molecular weights on the PDMS chains by changing the end groups. This suggests that the chain end modification affects the distribution of the chain ends, and the distribution induces a change in the local conformation near the free surface, which can be one of the contributors for the change observed in the surface tension.

Since the chain ends are segregated or depleted near the surface according to the chemical nature of the end group, the whole dimension of the chain is also affected by the chain end modification. The end-to-end distance is divided into two components in Figure 7a: the lateral ($R_{ee,xy}$) and perpendicular ($R_{ee,z}$). The ϵ for the end beads has its largest effect on the perpendicular component of those chains that have their center of mass near the midplane of the film. If such a chain is to place both of its ends near a surface, it is unlikely that it will do so by placing them both at the same surface; if it were to attempt to do so, it is unlikely that its center of mass could remain near the midplane. The more likely scenario is that one end will go to one surface and the other end will go to the other surface, producing a large perpendicular component for the end-to-end distance. This effect is strongest when ϵ is smallest, because the driving force for putting the ends near the surface is then the strongest. This effect should diminish strongly if the film becomes so thick that it cannot be spanned by the chain. Figure 7b shows the square of the radius of gyration in the lateral and perpendicular directions. On a relative basis, the influence of ϵ for the end beads is largest on $R^2_{g,z}$ for those chains with their center of masses near the midplane, due to the same effect.

For a short chain, the ratio $\langle R^2_{ee}\rangle/\langle R^2_g\rangle$ is larger than 6, and the crossover to the Gaussian statistics occurs around $n > 100$,[33] where n is the number of backbone carbon atoms. Figure 7c shows that chains with more attractive end groups show a lower value of $\langle R^2_{ee}\rangle/\langle R^2_g\rangle$, and the values are gradually decreasing as the chains go to the free surface. Unlike the effective range of the free surface found in the density profiles, the effect of the free surface in terms of the chain dimension exists in the entire region of the free film with thickness $4R_g$. Interestingly, the anisotropy in the chain dimension along the direction normal to the surface disappears in the case of $\epsilon = 350$, generating a wider plateau region in the middle of the film. At $\epsilon = 350$, the chain ends show less distinguishable end group segregation or depletion by canceling the free volume effect of chain ends with the relatively attractive end groups. The cancellation of the two factors might lead to the wider isotropic region in the middle of the film.

The molecular shape can be indexed by the relative shape anisotropy, κ^2, which is defined through asphericity and acylindricity. If there is an ellipsoidal object with the three squared principal moments, $L_1^2 > L_2^2 > L_3^2$, the squared radius of gyration, s^2, asphericity, b, and acylindricity, c, are defined as

$$s^2 = L_1^2 + L_2^2 + L_3^2 \tag{8}$$

$$b = L_1^2 - \frac{(L_2^2 + L_3^2)}{2} \tag{9}$$

$$c = L_2^2 - L_3^2 \tag{10}$$

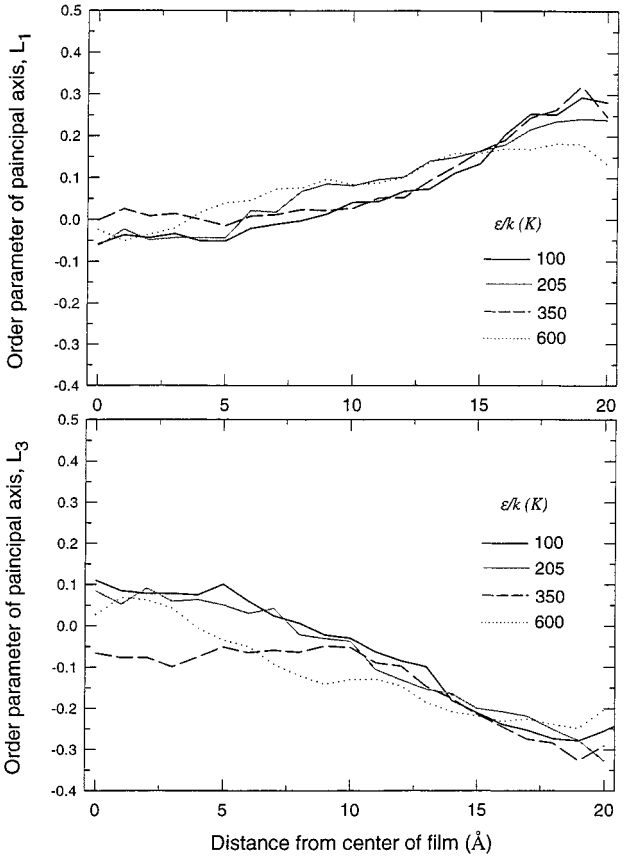

Figure 8. Order parameter of the (a) largest principal axis (L_1) and (b) smallest principal axis (L_3) of the chains in the freely standing films with four different end beads against the distance from the center of mass of the films.

Then the relative shape anisotropy is defined as

$$\kappa^2 = \frac{b^2 + {}^3/_4 c^2}{s^4} \tag{11}$$

The index, κ^2, should be 0 if the object is a perfect sphere and 1 if it is a perfect rod. The atactic polypropylene chain[34] gives a value of 0.41 for the κ^2. In the present simulations, the κ^2 is around 0.43−0.47 depending on the chemical modification of the chain ends. The more attractive chain end gives more spherical shape.

Having observed the dependence of the chain dimension and the chain shape on the nature of chain ends and the location of the chains in the film, we also looked into whether there is a preferred orientation of the chains. The order parameter is given by

$$S = \frac{\langle 3(\cos^2\theta) - 1\rangle}{2} \tag{12}$$

where θ is the angle between the principal axis and the direction normal to the film surface. The order parameter is 1 if the axis is parallel to the film surface and $-{}^1/_2$ if the axis is perpendicular to the film surface. For the completely random orientation, the value should be 0. In the middle region of the film, the L_1 and L_3 components show little evidence for order. Order is evident in the surface region, with $S_{L_1} > 0 > S_{L_3}$, as shown in Figure 8. Chains near the free surface have a tendency to be oriented parallel to the lateral direction, as found in earlier simulation.[15] The extent of the ordering does not change much with the chain end

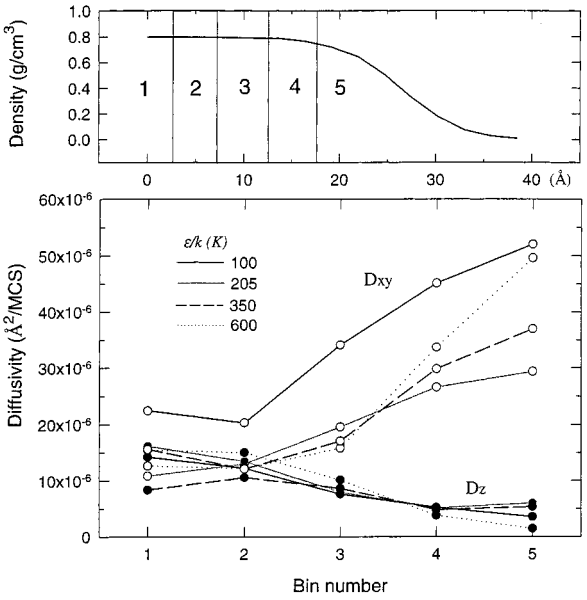

Figure 9. (a) Density profile of a freely standing film divided into five bins. (b) The *xy* directional (○) and the *z* directional (●) short-time diffusivity of the chains in the freely standing films as a function of bin number.

modification. However, in the case of $\epsilon = 350$, the results show a wider isotropic region in the middle of the film.

Dynamics. The dynamics of the thin films were examined by the diffusivity and the autocorrelation of the principal axis. The diffusivity is described by the short time self-diffusion obtained from the mean-square displacement vs MCS as defined by eqs 6 and 7. To achieve a statistical stability, the thin films were divided into five bins as shown in the top panel of Figure 9, and the average of the mean-square displacement of the chains located initially in each bin is considered. The two different directional diffusivities vs the bin location are plotted in the bottom panel of Figure 9. The diffusivities in the lateral direction (D_{xy}) and perpendicular direction (D_z) are not much different in the middle region of the film. The increase of the lateral directional mobility is taken accounted for the lower density. As one approaches the surface region, $D_{xy} \gg D_z$, but it is difficult to see any strong correlation of either diffusivity with ϵ. This independence from ϵ_{end} of the increase in D_{xy} in the surface region is consistent with the observation of a similar speed-up in simulations of cyclic chains, where there are no ends.[35]

Figure 10 gives the autocorrelation of the principal moments in time. The shape autocorrelation is given by

$$\frac{\langle L_i(0)\, L_i(t)\rangle - \langle L_i\rangle^2}{\langle L_i^2\rangle - \langle L_i\rangle^2} \tag{13}$$

where L_i is the ith principal moment of a chain. The largest component of the principal axis, L_1, decays much faster than the other two components no matter where the chains are. The chains with repulsive chain ends in the middle region (see top panel of Figure 10) show the fastest decay for L_1. The decay of the L_1 component near the surface did not depend on the chemical modification, but the decay of L_3 is clearly related to the chemical modification of chain ends (bottom panel of Figure 10). The more attractive chain end gives the slower decay of the shape autocorrelation. When the attractive chain

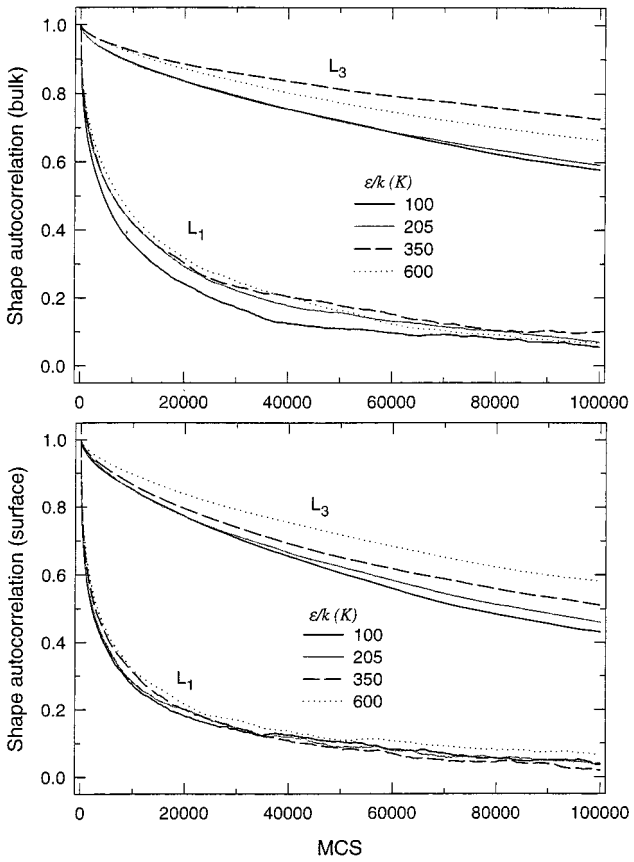

Figure 10. Shape autocorrelation of the chains in (a) the middle and (b) the surface region of the freely standing films. The L_1 and L_3 represent the largest and smallest principal moment, respectively.

ends prefer to go to the bulk region, they give an anchoring effect, which results in a slower shape fluctuation. This result suggests that the introduction of a repulsive group to the chain end can induce a faster dynamics of the chains.

Conclusions

The effect of the chain end modification in a freely standing film has been studied by a Monte Carlo simulation on a high coordination lattice. The rotational isomeric state model is incorporated as the short-range interaction and Lennard-Jones potential is used for the long-range interaction. The computationally efficient method is applied to the series of polyethylene melts, and the chain end modification is made by changing the ϵ value of the chain end beads from attractive to repulsive compared to the middle beads. The important findings of this study are summarized as follows.

(1) The film thickness should be larger than $\sim 4R_g$ to achieve a bulk density in the middle of the freely standing film. For the thinner film of $\sim 2R_g$ thickness, the maximum internal density does not show a dependence on the nature of the chain ends, while for the film of $\sim 4R_g$ thickness, the maximum density increases with more attractive chain ends. The density profiles are well fitted to the hyperbolic equations originally developed for a binary immiscible blend, regardless of the nature of chain ends.

(2) The chain ends that have ϵ values no larger than those of middle bead prefer to go to the free surface. However, the sufficiently attractive chain ends (large ϵ) are depleted near the free surface. The population shows an oscillation with $\sim 2R_g$ period, and the oscillation is intensified as the energy difference between chain ends and middle group gets larger.

(3) The population of the conformation of pairs of bonds is in the order of (tg^+,tg^-,g^+t,g^-t) > tt > (g^+g^+,g^-g^-) > (g^+g^-,g^-g^+). In the middle of the film, the population does not vary much with chain end modification. However, in the free surface region, more gauche conformations are found in the films with more attractive chain ends. The higher population of the gauche conformation produces a higher chain conformational energy, which can contribute to the higher surface tension of the films with the highly attractive chain ends observed in experiment.[10]

(4) The chain dimension examined by end-to-end distance and radius of gyration reveals an anisotropy along the direction normal to film surface in most cases. The end-to-end distance of the chains with repulsive chain ends is the highest value resulting from the chain end segregation. For the relatively attractive chain ends, a wider isotropic region in terms of the chain dimension is observed, which is the result of the cancellation of the two effects: the entropy effect to prefer to a free surface due to the less entropic penalty of the chain ends and the enthalpic effect to prefer bulk region due to the attractive nature of the chain ends. This trend is also observed from the shape anisotropy and order parameter of the radius of gyration tensor.

(5) From the dynamics study by looking at the chain diffusivity and shape fluctuation, the repulsive chain ends induce a faster dynamics in the middle region of the freely standing film. The similar effect is also observed for the chains in the free surface region. However, the mobility of chains near surface along the normal direction to the film surface is greatly reduced due to the strong confinement against vacuum surface, while the lateral mobility is increased around 3 times compared to that in the bulk region regardless of the nature of the chain ends.

Acknowledgment. This work was supported by the National Science Foundation. (Grants DMR-95-23278 and DMR-98-44069).

References and Notes

(1) de Gennes, P. G. *Scaling Concepts in Polymer Physics*; Cornell University Press: Ithaca, New York, 1979.
(2) Doi, M.; Edwards, S. F. *The Theory of Polymer Dynamics*; Clarendon Press: Oxford, U.K., 1986.
(3) von Meerwall, E.; Beckman, S.; Jang, J. H.; Mattice, W. L. *J. Chem. Phys.* **1998**, *108*, 4299.
(4) Horinaka, J.; Maruta, M.; Ito, S.; Yamamoto, M. *Macromolecules* **1999**, *32*, 1134.
(5) Ferry, J. D. *Viscoelastic Properties of Polymers*, 3rd ed.; Wiley and Sons: New York, 1980.
(6) Elman, J. F.; Johs, B. D.; Long, T. E.; Koberstein, J. T. *Macromolecules* **1994**, *27*, 5341.
(7) Mayes, A. M. *Macromolecules* **1994**, *27*, 3114.
(8) Kajiyama, T.; Tanaka, K.; Takahara, A. *Macromolecules* **1997**, *30*, 280.
(9) Tanaka, K.; Jiang, X.; Nakamura, K.; Takahara, A.; Kajiyama, T.; Ishizone, T.; Hirao, A.; Nakahama, S. A. *Macromolecules* **1998**, *31*, 5148.
(10) Jalbert, C.; Koberstein, J. T.; Yilgor, I.; Gallagher, P.; Krukonis, V. *Macromolecules* **1993**, *26*, 3069.
(11) Henn, G.; Bucknall, D. G.; Stamm, M.; Vanhoorne, P.; Jérôme, R. *Macromolecules* **1996**, *29*, 4305.
(12) Schaub, T. F.; Kellogg, G. J.; Mayes, A. M.; Kulasekere, R.; Ankner, J. F.; Kaiser, H. *Macromolecules* **1996**, *29*, 3982.
(13) Iijima, M.; Nagasaki, Y.; Okada, T.; Kato, M.; Kataoka, K. *Macromolecules* **1999**, *32*, 1140.
(14) Jannasch, P. *Macromolecules* **1998**, *31*, 1341.

(15) Doruker, P.; Mattice, W. L. *Macromolecules* **1998**, *31*, 1418.
(16) Jang, J. H.; Mattice, W. L. *Polymer* **1999**, *40*, 4685.
(17) Jang, J. H.; Mattice, W. L. *Macromolecules* **2000**, *33*, 1467.
(18) Rapold, R. F.; Mattice, W. L. *J. Chem. Soc., Faraday Trans.* **1995**, *91*, 2435.
(19) Cho, J.; Mattice, W. L. *Macromolecules* **1997**, *30*, 637.
(20) Baschnagel, J.; Binder, K.; Doruker, P.; Gusev, A. A.; Hahn, O.; Kremer, K.; Mattice, W. L.; Müller-Plathe, F.; Murat, M.; Paul, W.; Santos, S.; Suter, U. W.; Tries, V. *Adv. Polym. Sci.* **2000**, *152*, 41.
(21) Metropolis, N.; Rosenbluth, A. W.; Rosenbluth, M. N.; Teller, A. H.; Teller, E. *J. Chem. Phys.* **1953**, *21*, 1087.
(22) Mattice, W. L.; Suter, U. W. *Conformational Theory of Large Molecules. The Rotational Isomeric State Model in Macromolecular Systems;* Wiley: New York, 1994.
(23) Abe, A.; Jernigan, R. L.; Flory, P. J. *J. Am. Chem. Soc.* **1966**, *88*, 631.
(24) Misra, S.; Flemming, P. D., III; Mattice, W. L. *J. Comput.-Aided Mater. Des.* **1995**, *2*, 101.
(25) Mansfield, K. F.; Theodorou, D. N. *Macromolecules* **1991**, *24*, 6283.
(26) Lin, E. K.; Wu, W. L.; Satija, S. K. *Macromolecules* **1997**, *30*, 7224.
(27) Frank, B.; Gast, A. P.; Russell, T. P.; Brown, H. R.; Hawker, C. *Macromolecules* **1996**, *29*, 6531.
(28) Helfand, E.; Tagami, Y. *J. Chem. Phys.* **1971**, *56*, 3592.
(29) Helfand, E.; Tagami, Y. *J. Chem. Phys.* **1972**, *57*, 1812.
(30) Wu, D. T.; Fredrickson, G. H.; Carton, J.; Ajdari, A.; Leibler, L. *J. Polym. Sci., Part B: Polym. Phys.* **1995**, *33*, 2373.
(31) Kumar, S. K.; Vacatello, M.; Yoon, D. Y. *J. Chem. Phys.* **1988**, *89*, 5209.
(32) Kumar, S. K.; Vacatello, M.; Yoon, D. Y. *Macromolecules* **1990**, *23*, 2189.
(33) Paul, W.; Smith, G. D.; Yoon, D. Y. *Macromolecules* **1997**, *30*, 7772.
(34) Theodorou, D. N.; Suter, U. W. *Macromolecules* **1985**, *18*, 1206.
(35) Doruker, P.; Mattice, W. L. *J. Phys. Chem. B* **1999**, *103*, 178.

MA000957M